2014 IEEE International Conference on Robotics & Automation (ICRA)
Hong Kong Convention and Exhibition Center
May 31 - June 7, 2014. Hong Kong, China

A new method for parameter identification for N-DOF hydraulic robots

Satoru Sakai[1] and Yuzo Maeshima[1]

***Abstract*— Parameter identification for N-DOF hydraulic robots (e.g., BigDog, PETMAN and developing automated excavators) is not an old problem at all. Indeed, recent papers still identify difficult parameters (the bulk modulus and the flow gain coefficients) by trial and error. This paper is the first report to solve this problem. First, new structural properties of hydraulic robots are found in comparison with electric robots and then the drawbacks of the conventional methods are discussed. Second, by modifying one of the conventional methods, a scientific method is proposed and applied to an actual hydraulic manipulator. Third, the validity of the proposed method is confirmed by model validation. Remarkably, the difficult parameters are identified very well without any trial and error. The proposed method is applicable to electric robots even on the unknown inclination.**

I. INTRODUCTION

Hydraulic robots are gaining popularity in robotics and automation such as in the field of construction, agriculture, demining and rescue and so on. However, in comparison with electric robots, hydraulic robots need experiment and skip numerical simulation due to a lack of the modeling. Not only numerical simulation but also model based control (e.g., impedance control, adaptive control) are few. Since the modeling is a foundation of design optimizations, currently, it is one of the serious robotics problems to develop the good procedure of the modeling.

Of course, the state space expression of hydraulic robots is already known but the modeling needs the parameter identification. In fact, even in recent papers on hydraulic robots and the other hydraulic systems [7],[2],[9], difficult parameters (the bulk modulus and the flow gain coefficients) are identified by trial and error [8],[1],[10],[3].

Unfortunately, the difficulty of the parameter identification for hydraulic robots is not discussed clearly so far. Table I gives new structural properties of hydraulic robots to explain the difficulty whose details are discussed later again. First, since the states do not always exist for a certain set of the initial states and the parameters, *the search methods* such as PSO (Particle Swam Optimization) [5] and GA (Genetic Algorithm) do not work because numerical simulation in the methods just runs as long as the states exist. Second, since there exists an unknown common parameter which is newly defined as a parameter independent from the joint number, *the conventional sequential method* [6] does not guarantee the uniqueness.

TABLE I

NEW STRUCTURAL PROPERTIES OF HYDRAULIC ROBOTS

Controlled model	States	Common parameters Unknown	Common parameters Known
Hydraulic	**not always exist**	**exist,** b	exist, g
Electric*	always exist	not exist	exist, g

* = "An electric robot is equivalent to a rigid body robot if both the elastic and the electric energy storing and dissipative elements are negligible. "

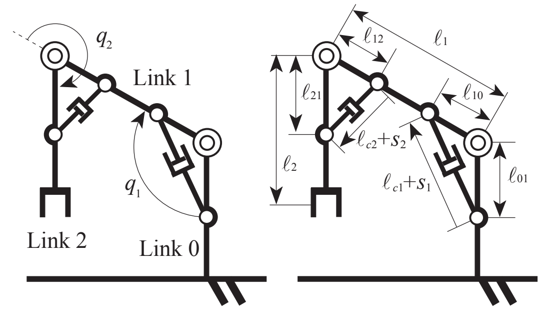

Fig. 1. Hydraulic robot.

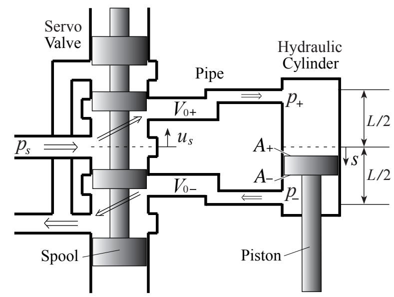

Fig. 2. Hydraulic actuator.

The proposed method in this paper identifies the parameter without running any numerical simulation and guarantees the uniqueness by paying attention to Hilbert space. The rest of this paper is organized as follows. In Section II, a review of hydraulic robots are provided and the details of new structural properties are discussed. In Section III, the proposed method is discussed and in Section IV, the proposed method is applied to an actual experimental setup. In Section V, the validity of the proposed method is confirmed in several conditions. Finally, Section VI concludes this paper.

II. NEW STRUCTURAL PROPERTY

A. A review of state space expression

Let us start to review hydraulic robots from the viewpoint of the parameter identification. Without loss of generality,

[1] Satoru Sakai is with Department of Mechanical Engineering, Shinshu University, Nagano, Japan satorus@shinshu-u.ac.jp

this paper discusses the 2-DOF case only as shown in Figs.1,2. A hydraulic robot is described by

$$\dot{x} = f_0(x) + g_0(x)u,\ \ y = x \tag{1}$$

with

$$x := [(q_1\ q_2)\ \ (\dot{q}_1\ \dot{q}_2)\ \ (p_{+1}\ p_{+2})\ \ (p_{-1}\ p_{-2})]^{\mathrm{T}}, u := [u_{s1}\ u_{s2}]^{\mathrm{T}}$$

where q_i is the joint angle, $\dot{q}_i$ is the joint angle velocity, p_{+i} is the one-side pressure (the head side pressure), p_{-i} is another side pressure (the rod side pressure), and the input u_{si} is the spool displacement. The drift term f_o and the input term $g_o(x)u$ are defined as follows.

$$f_0(x) = \begin{bmatrix} (\dot{q}_1\ \dot{q}_2)^{\mathrm{T}} \\ -M^{-1}(q)\left(C(q,\dot{q})\dot{q} + F_v\dot{q} + g(q) - G(q)^{-\mathrm{T}}F(x)\right) \\ (f_{+1}(x)\ f_{+2}(x))^{\mathrm{T}} \\ (f_{-1}(x)\ f_{-2}(x))^{\mathrm{T}} \end{bmatrix}$$

$$g_0(x) = \begin{bmatrix} \begin{pmatrix} 0 & 0 \\ 0 & 0 \end{pmatrix} \\ \begin{pmatrix} 0 & 0 \\ 0 & 0 \end{pmatrix} \\ \begin{pmatrix} g_{+1}(x) & 0 \\ 0 & g_{+2}(x) \end{pmatrix} \\ \begin{pmatrix} g_{-1}(x) & 0 \\ 0 & g_{-2}(x) \end{pmatrix} \end{bmatrix}$$

$$\begin{aligned}
M(q) &= \begin{bmatrix} M_1 + 2R_{12}\cos(q_2) & M_2 + R_{12}\cos(q_2) \\ M_2 + R_{12}\cos(q_2) & M_2 \end{bmatrix} \\
C(q,\dot{q}) &= \begin{bmatrix} -2R_{12}\dot{q}_1\dot{q}_2\sin(q_2) - R_{12}\dot{q}_2^2\sin(q_2) \\ R_{12}\dot{q}_1^2\sin(q_2) \end{bmatrix} \\
F_v &= \begin{bmatrix} F_{v1} & 0 \\ 0 & F_{v2} \end{bmatrix} \\
g(q) &= \begin{bmatrix} W_1 g\sin(q_1) + W_2 g\sin(q_1+q_2) \\ W_2 g\sin(q_1+q_2) \end{bmatrix} \\
G(q)^{-\mathrm{T}} &= \begin{bmatrix} G_{11}(q_1) & 0 \\ 0 & G_{22}(q_2) \end{bmatrix} \\
F(x) &= \begin{bmatrix} A_{+1}p_{+1} - A_{-1}p_{-1} \\ A_{+2}p_{+2} - A_{-2}p_{-2} \end{bmatrix} \\
f_{+i}(x) &= \frac{b}{V_{+i}(s_i)}\left(-A_{+i}\dot{s}_i\right)\ ,\ f_{-i}(x) = \frac{b}{V_{-i}(s_i)}\left(+A_{-i}\dot{s}_i\right) \\
g_{+i}(x) &= \frac{b}{V_{+i}(s_i)}\left(+C_{f++i}h_{++i}(p_{+i}) + C_{f+-i}h_{+-i}(p_{+i})\right) \\
g_{-i}(x) &= \frac{b}{V_{-i}(s_i)}\left(-C_{f-+i}h_{-+i}(p_{-i}) - C_{f--i}h_{--i}(p_{-i})\right)
\end{aligned}$$

$$\begin{aligned}
M_1 &= I_1 + I_2 + m_1\ell_{g1}^2 + m_2\left(\ell_1^2 + \ell_{g2}^2\right) \\
M_2 &= I_2 + m_2\ell_{g2}^2 \\
R_{12} &= m_2\ell_{g2}\ell_1, W_1 = m_1\ell_{g1} + m_2\ell_1, W_2 = m_2\ell_{g2} \\
G_{11} &= \frac{\ell_{01}\ell_{10}\sin(q_1)}{\ell_{c1} + s_1(q_1)}, G_{22} = \frac{\ell_{12}\ell_{21}\sin(q_2 - \pi)}{\ell_{c2} + s_2(q_2)} \\
V_{+i}(s_i) &= V_{0+i} + (L_i/2 + s_i)A_{+i} \\
V_{-i}(s_i) &= V_{0-i} + (L_i/2 - s_i)A_{-i} \\
h_{++i}(p_{+i}) &:= \begin{cases} \sqrt{-p_{+i} + p_s} & (u_{si} > 0) \\ 0 & (u_{si} \le 0) \end{cases} \\
h_{+-i}(p_{+i}) &:= \begin{cases} 0 & (u_{si} \ge 0) \\ \sqrt{+p_{+i}} & (u_{si} < 0) \end{cases} \\
h_{-+i}(p_{-i}) &:= \begin{cases} \sqrt{+p_{-i}} & (u_{si} > 0) \\ 0 & (u_{si} \le 0) \end{cases} \\
h_{--i}(p_{-i}) &:= \begin{cases} 0 & (u_{si} \ge 0) \\ \sqrt{-p_{-i} + p_s} & (u_{si} < 0) \end{cases}
\end{aligned}$$

where the subscript $i = 1$ or 2 is the joint number and the subscript $+$ or $-$ denotes the head side and the rod side, respectively with the link mass m_i, the link interia of moment around the center of the gravity I_i, the friction coefficient F_{vi}, the gravity acceleration g, the link length ℓ_i, the distance between the joint center and the center of the gravity ℓ_{gi}, the piston minimal length ℓ_{ci}, the distance between the joint center and the piston endpoint ℓ_{ij}, the bulk modulus b, the flow gain coefficient $C_{f\pm\pm i}$, the stroke L_i, the piston areas $A_{\pm i}$, the pipe volume $V_{0\pm i}$, and the pump supply pressure p_s. The symbol denotes the piston displacement $s_i \in \mathrm{R}$ and the matrix components $G_{ii}(q)$ is the cylinder Jacobian. The origin of the piston displacement s_i, the spool displacement u_i, the cylinder pressure $p_\pm$ are the middle point of the stroke range, the normal position, air pressure, respectively.

The model above is not as precise as many models in fluid dynamics but is associated with unknown parameter perturbation and uncertainty.

B. Structural properties

This subsection discusses the difficulty of parameter identification based on new structural properties of hydraulic robots as shown in Table I.

First, the states x of Equation (1) do not always exist as real number. For a certain set of the initial states and the parameters, the state x can be complex number due to the square function in the input term $g_0(x)u$. Of course, the actual hydraulic robots do not make the states complex number, but Equation (1) is based on many assumptions.

Since the search methods such as PSO and GA repeat numerical simulation and automatic parameter tuning by turns, if the states x do not exist, numerical simulation stops and the search methods fail immediately.

Second, a certain parameter is unknown but exists in all links in case of hydraulic robots, unlike electric robots. In general, robot parameters are classified into:
P1) the parameters not depending on the joint number,
P2) the parameters depending on the joint number.

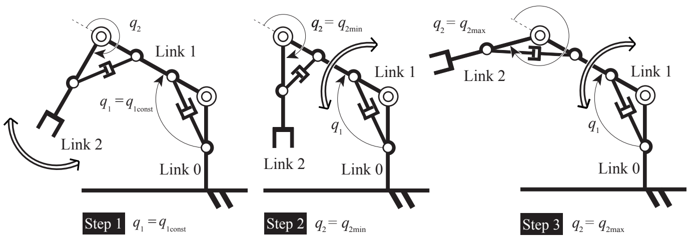

Fig. 3. Conceptual diagram of the sequential method.

The former exist in all links and thus are defined as *common parameter* in this paper. In vertical cases, the gravity acceleration g exists in all links of electric robots and the bulk modulus b is also exists in all links of hydraulic robots. However, only the bulk modulus b is unknown and needs the parameter identification but the gravity acceleration g is usually known as 9.8 $[\mathrm{m/s^2}]$. In horizontal cases, the bulk modulus b still exists in hydraulic robots even though the gravity acceleration g does not exist.

Fig. 3 shows an example of the sequential procedure consisting of three steps here. Since the conventional sequential method identifies a part of the full parameters between each steps, the uniqueness is not guaranteed in N-DOF cases. For example, some parameters are identified between STEP1 and STEP2 but one of them is again identified between STEP2 and STEP3.

This new problem of the conventional sequential method may not serious in case of electric robots because a certain coordinate transformation (e.g., from the relative joint angle to the absolute joint angle), may make each parameter appear at only one of these steps. However, in case of hydraulic robots, since an common parameter appear at all steps for any coordinate transformation, if the common parameter is unknown, the conventional sequential method fails to guarantee the uniqueness.

TABLE II

MEASURED PARAMETERS AND UNKNOWN PARAMETERS.

Parameter	Symbol	Unit	Value
Inertia parameter	M_i	$\mathrm{kgm^2}$	Unknown
Inertia parameter	R_{12}	$\mathrm{kgm^2}$	Unknown
Damping coefficient	F_{vi}	Ns/m	Unknown
Gravity parameter	W_i	kgm	Unknown
Bulk modulus	b	MPa	Unknown
Flow gain coefficient	$C_{f\pm\pm i}$	$\mathrm{m^2/(sV\sqrt{Pa})}$	Unknown
Gravity acceleration	g	$\mathrm{m/s^2}$	9.8
Standard length of piston	ℓ_i	m	5.0×10^{-1}
Standard length of piston	ℓ_{ci}	m	3.0×10^{-1}
Piston attachment position	ℓ_{01}	m	1.1×10^{-1}
Piston attachment position	ℓ_{10}	m	3.3×10^{-1}
Piston attachment position	ℓ_{12}	m	2.7×10^{-1}
Piston attachment position	ℓ_{21}	m	1.0×10^{-1}
Stroke	L_i	m	7.5×10^{2}
Cap area	A_{+i}	$\mathrm{m^2}$	7.0×10^{-4}
Rod area	A_{-i}	$\mathrm{m^2}$	5.4×10^{-4}
Pipe volume	$V_{0\pm1}$	$\mathrm{m^3}$	7.9×10^{-5}
Pipe volume	$V_{0\pm2}$	$\mathrm{m^3}$	6.3×10^{-5}
Pump supply pressure	p_s	Pa	$7.0\times10^{+6}$

Remark One may use the following calculations:
E1) Identify the unknown parameter at only one step and use the parameter as a known parameter.
E2) Identify the unknown parameter at every step and take the average after all steps finish.
However, since the former uses the only part of the total data and the latter has a different sense from the identification of the other parameters, both calculations are never scientific.

Remark Suppose two normal equations $A_i x_i = b_i,\ x_i \in \mathbb{R}^2,\ i \in \{1,2\}$ and assume that the second component of x_1 and the first component of x_2 are the same (i.e., $x_{12} = x_{21}$). Then a coupling of the normal equations is equivalent to a linear equation $Ax = b$ with $x = [x_{11}, x_{12}, x_{22}]^{\mathrm{T}}$. Furthermore, any component of the solution x_i of the normal equation is not equivalent to all components of the solution x of the linear equation.

III. Full Parameter Identification

In order to solve the problems of all of the conventional methods, by modifying the conventional sequential method from the viewpoint of Hilbert space, the proposed method uses the whole of the total data and has the same sense as the identification of the other parameters.

$<$ **STEP1** $>$ The joint 1 is fixed ($q_1 = q_{1\mathrm{const}}, \dot q_1 = \ddot q_1 = 0$) and the joint 2 is driven. It is not possible to see the state equation (1) as a linear equation with respect to the unknown parameters, unlike that of electric robots. However, after the following procedure, 1) multiply the matrix $M(s)$ to the both sides from the left in the second equation to define the drift term f_0, 2) multiply the scalar V_{+i}/b to the both sides in the third equation, 3) multiply the scalar V_{+-}/b to the both sides in the forth equation, the state space equation is of the form of the linear equation with non-zero right hand.

$$\begin{aligned} M_2\ddot q_2(t)+F_{v2}\dot q_2(t) \quad &+ \quad W_2 g\sin(q_{1\mathrm{const}}+q_2(t)) \\ &= \quad G_{22}(q_2(t))^{-1}(A_{+2}p_{+2}(t)-A_{-2}p_{-2}(t)) \end{aligned}$$

$$\rightarrow \begin{bmatrix} \sigma_{11}(t) & \sigma_{12}(t) & \sigma_{13}(t) \end{bmatrix} \begin{bmatrix} M_2 \\ F_{v2} \\ W_2 \end{bmatrix} = \begin{bmatrix} f_{11}(t) \end{bmatrix},$$

with

$$\begin{aligned} \sigma_{11}(t) &= \ddot q_2(t)\ ,\ \sigma_{12}(t) = \dot q_2(t)\ ,\ \sigma_{13}(t) = g\sin(q_{1\mathrm{const}}+q_2(t)) \\ f_{11}(t) &= G_{22}(q_2(t))^{-1}\left(A_{+2}p_{+2}(t) - A_{-2}p_{-2}(t)\right) \end{aligned}$$

and

$$\begin{cases} -\frac{1}{b}\dot p_{+2}(t)V_{+2}(t) + C_{f++2}h_{++2}(t)u_{s2}(t) \\ \qquad\qquad +C_{f+-2}h_{+-2}(t)u_{s2}(t) = +A_{+2}\dot s_2(t) \\ -\frac{1}{b}\dot p_{-2}(t)V_{-2}(t) - C_{f-+2}h_{-+2}(t)u_{s2}(t) \\ \qquad\qquad -C_{f--2}h_{--2}(t)u_{s2}(t) = -A_{-2}\dot s_2(t) \end{cases}$$

$$\rightarrow \begin{bmatrix} \varepsilon_{11}(t) & \varepsilon_{12}(t) & \varepsilon_{13}(t) & 0 & 0 \\ \varepsilon_{21}(t) & 0 & 0 & \varepsilon_{24}(t) & \varepsilon_{25}(t) \end{bmatrix} \begin{bmatrix} 1/b \\ C_{f++2} \\ C_{f+-2} \\ C_{f-+2} \\ C_{f--2} \end{bmatrix} = \begin{bmatrix} f_{21}(t) \\ f_{22}(t) \end{bmatrix},$$

with

$$\begin{aligned} \varepsilon_{11}(t) &= -\dot p_{+2}(t)V_{+2}(t) \quad , \quad \varepsilon_{21}(t) = -\dot p_{-2}(t)V_{-2}(t) \\ \varepsilon_{12}(t) &= +h_{++2}(t)u_{s2}(t) \quad , \quad \varepsilon_{13}(t) = +h_{+-2}(t)u_{s2}(t) \\ \varepsilon_{24}(t) &= -h_{-+2}(t)u_{s2}(t) \quad , \quad \varepsilon_{25}(t) = -h_{--2}(t)u_{s2}(t) \\ f_{21}(t) &= +A_{+2}\dot s_2(t) \quad , \quad f_{22}(t) = -A_{-2}\dot s_2(t) \end{aligned}$$

Note that the above linear equations are quite lucky because the right hand sides f_{11}, f_{21}, f_{22} are not unknown and also not zeros. Otherwise, the unknown parameters are identified as just zero which are clearly incorrect. Unlike the conventional sequential procedure, let us go to the next step immediately without solving the above normal equation.

$<$ **STEP2** $>$ The joint 2 is fixed at the minimal values ($q_2 = q_{2\min}, \dot{q}_2 = \ddot{q}_2 = 0$), and the joint 1 is driven.

$$\begin{aligned}&(M_1 + 2R_{12}\cos(q_{2\min}))\ddot{q}_1(t) + F_{v1}\dot{q}_1(t) + W_1 g\sin(q_1(t))\\&+W_2 g\sin(q_1(t)+q_{2\min}) = G_{11}(q_1(t))^{-1}(A_{+1}p_{+1}(t) - A_1 p_1(t))\end{aligned}$$

with

$$\rightarrow \begin{bmatrix} \phi_{11}(t) & \phi_{12}(t) & \phi_{13}(t) & \phi_{14}(t) & \phi_{15}(t) \end{bmatrix} \begin{bmatrix} M_1 \\ R_{12} \\ F_{v1} \\ W_1 \\ W_2 \end{bmatrix} = \begin{bmatrix} f_{12}(t) \end{bmatrix},$$

$$\begin{aligned}\phi_{11}(t) &= \ddot{q}_1(t)\ ,\ \phi_{12}(t) = 2\ddot{q}_1(t)\cos(q_{2\min})\ ,\ \phi_{13}(t) = \dot{q}_1(t)\\ \phi_{14}(t) &= g\sin(q_1(t))\ ,\ \phi_{15}(t) = g\sin(q_1(t)+q_{2\min})\\ f_{12}(t) &= G_{11}(q_1(t))^{-1}(A_{+1}p_{+1}(t) - A_{-1}p_{-1}(t))\end{aligned}$$

and

$$\begin{cases} -\frac{1}{b}\dot{p}_{+1}(t)V_{+1}(t) + C_{f++1}h_{++1}(t)u_{s1}(t) \\ \qquad\qquad +C_{f+-1}h_{+-1}(t)u_{s1}(t) = +A_{+1}\dot{s}_1(t) \\ -\frac{1}{b}\dot{p}_{-1}(t)V_{-1}(t) - C_{f-+1}h_{-+1}(t)u_{s1}(t) \\ \qquad\qquad -C_{f--1}h_{--1}(t)u_{s1}(t) = -A_{-1}\dot{s}_1(t) \end{cases}$$

$$\rightarrow \begin{bmatrix} \lambda_{11}(t) & \lambda_{12}(t) & \lambda_{13}(t) & 0 & 0 \\ \lambda_{21}(t) & 0 & 0 & \lambda_{24}(t) & \lambda_{25}(t) \end{bmatrix} \begin{bmatrix} \frac{1}{b} \\ C_{f++1} \\ C_{f+1} \\ C_{f+1} \\ C_{f-1} \end{bmatrix} = \begin{bmatrix} f_{23}(t) \\ f_{24}(t) \end{bmatrix},$$

with

$$\begin{aligned}\lambda_{11}(t) &= -\dot{p}_{+1}(t)V_{+1}(t)\ ,\ \lambda_{21}(t) = -\dot{p}_1(t)V_1(t)\\ \lambda_{12}(t) &= +h_{++1}(t)u_{s1}(t)\ ,\ \lambda_{13}(t) = +h_{+-1}(t)u_{s1}(t)\\ \lambda_{24}(t) &= -h_{-+1}(t)u_{s1}(t)\ ,\ \lambda_{25}(t) = -h_{--1}(t)u_{s1}(t)\\ f_{23}(t) &= +A_{+1}\dot{s}_1(t)\ ,\ f_{24}(t) = -A_{-1}\dot{s}_1(t)\end{aligned}$$

As in STEP1, the right hand sides are not unknown and also not zeros and thus let us go to the next step again.

$<$ **STEP3** $>$ The joint 2 is fixed at the maximal values ($q_2 = q_{2\max}, \dot{q}_2 = \ddot{q}_2 = 0$), and the joint 1 is driven.

$$\begin{aligned}&(M_1 + 2R_{12}\cos(q_{2\max}))\ddot{q}_1(t) + F_{v1}\dot{q}_1(t) + W_1 g\sin(q_1(t))\\&+W_2 g\sin(q_1(t)+q_{2\max}) = G_{11}(q_1(t))^{-1}(A_{+1}p_{+1}(t) - A_{-1}p_{-1}(t))\end{aligned}$$

$$\rightarrow \begin{bmatrix} \omega_{11}(t) & \omega_{12}(t) & \omega_{13}(t) & \omega_{14}(t) & \omega_{15}(t) \end{bmatrix} \begin{bmatrix} M_1 \\ R_{12} \\ F_{v1} \\ W_1 \\ W_2 \end{bmatrix} = \begin{bmatrix} f_{13}(t) \end{bmatrix},$$

$$\begin{aligned}\omega_{11}(t) &= \ddot{q}_1(t)\ ,\ \omega_{12}(t) = 2\ddot{q}_1(t)\cos(q_{2\max})\ ,\ \omega_{13}(t) = \dot{q}_1(t)\\ \omega_{14}(t) &= g\sin(q_1(t))\ ,\ \omega_{15}(t) = g\sin(q_1(t)+q_{2\max})\\ f_{13}(t) &= G_{11}(q_1(t))^{-1}(A_{+1}p_{+1} - A_{-1}p_{-1})\end{aligned}$$

$$\begin{cases} -\frac{1}{b}\dot{p}_{+1}(t)V_{+1}(t) + C_{f++1}h_{++1}(t)u_{s1}(t) \\ \qquad\qquad +C_{f+-1}h_{+-1}(t)u_{s1}(t) = +A_{+1}\dot{s}_1(t) \\ -\frac{1}{b}\dot{p}_{-1}(t)V_{-1}(t) - C_{f-+1}h_{-+1}(t)u_{s1}(t) \\ \qquad\qquad -C_{f--1}h_{--1}(t)u_{s1}(t) = -A_{-1}\dot{s}_1(t) \end{cases}$$

$$\rightarrow \begin{bmatrix} \rho_{11}(t) & \rho_{12}(t) & \rho_{13}(t) & 0 & 0 \\ \rho_{21}(t) & 0 & 0 & \rho_{24}(t) & \rho_{25}(t) \end{bmatrix} \begin{bmatrix} 1/b \\ C_{f++1} \\ C_{f+-1} \\ C_{f-+1} \\ C_{f--1} \end{bmatrix} = \begin{bmatrix} f_{25}(t) \\ f_{26}(t) \end{bmatrix},$$

$$\begin{aligned}\rho_{11}(t) &= -\dot{p}_{+1}(t)V_{+1}(t)\ ,\ \rho_{21}(t) = -\dot{p}_{-1}(t)V_{-1}(t)\\ \rho_{12}(t) &= +h_{++1}(t)u_{s1}(t)\ ,\ \rho_{13}(t) = +h_{+-1}(t)u_{s1}(t)\\ \rho_{24}(t) &= -h_{-+1}(t)u_{s1}(t)\ ,\ \rho_{25}(t) = -h_{-1}(t)u_{s1}(t)\\ f_{25}(t) &= +A_{+1}\dot{s}_1(t)\ ,\ f_{26}(t) = -A_{-1}\dot{s}_1(t)\end{aligned}$$

STEP3 is the almost same as the STEP2 but used to explain the following final step.

$<$ **STEP4** $>$ A part of the unknown parameters, namely $b, C_{f\pm\pm1}, M_1, R_{12}, F_{v1}, W_1, W_2$ appears twice or more. Especially, the bulk modulus b will appear in every steps and is not identified uniquely for all coordinate transformation.

In this step, first let us couple all of the normal equations into the following smaller normal equations.

$$X_{1N}\underbrace{\begin{bmatrix} M_1 \\ M_2 \\ R_{12} \\ F_{v1} \\ F_{v2} \\ W_1 \\ W_2 \end{bmatrix}}_{a_1} = Y_{1N}\quad ,\quad X_{2N}\underbrace{\begin{bmatrix} \frac{1}{b} \\ C_{f++1} \\ C_{f+-1} \\ C_{f-+1} \\ C_{f--1} \\ C_{f++2} \\ C_{f+-2} \\ C_{f-+2} \\ C_{f--2} \end{bmatrix}}_{a_2} = Y_{2N} \qquad (2)$$

with

$$X_{1N} = \begin{bmatrix} 0 & \sigma_{11}(t_1) & 0 & 0 & \sigma_{12}(t_1) & 0 & \sigma_{13}(t_1) \\ \phi_{11}(t_1) & 0 & \phi_{12}(t_1) & \phi_{13}(t_1) & 0 & \phi_{14}(t_1) & \phi_{15}(t_1) \\ \omega_{11}(t_1) & 0 & \omega_{12}(t_1) & \omega_{13}(t_1) & 0 & \omega_{14}(t_1) & \omega_{12}(t_1) \\ \vdots & \vdots & \vdots & \vdots & \vdots & \vdots & \vdots \\ 0 & \sigma_{11}(t_N) & 0 & 0 & \sigma_{12}(t_N) & 0 & \sigma_{13}(t_N) \\ \phi_{11}(t_N) & 0 & \phi_{12}(t_N) & \phi_{13}(t_N) & 0 & \phi_{14}(t_N) & \phi_{15}(t_N) \\ \omega_{11}(t_N) & 0 & \omega_{12}(t_N) & \omega_{13}(t_N) & 0 & \omega_{14}(t_N) & \omega_{15}(t_N) \end{bmatrix}$$

and

$$X_{2N} = \begin{bmatrix} \varepsilon_{11}(t_1) & 0 & 0 & 0 & 0 & \varepsilon_{12}(t_1) & \varepsilon_{13}(t_1) & 0 & 0 \\ \varepsilon_{21}(t_1) & 0 & 0 & 0 & 0 & 0 & 0 & \varepsilon_{24}(t_1) & \varepsilon_{25}(t_1) \\ \lambda_{11}(t_1) & \lambda_{12}(t_1) & \lambda_{13}(t_1) & 0 & 0 & 0 & 0 & 0 & 0 \\ \lambda_{21}(t_1) & 0 & 0 & \lambda_{24}(t_1) & \lambda_{25}(t_1) & 0 & 0 & 0 & 0 \\ \rho_{11}(t_1) & \rho_{12}(t_1) & \rho_{13}(t_1) & 0 & 0 & 0 & 0 & 0 & 0 \\ \rho_{21}(t_1) & 0 & 0 & \rho_{24}(t_1) & \rho_{25}(t_1) & 0 & 0 & 0 & 0 \\ \vdots & \vdots & \vdots & \vdots & \vdots & \vdots & \vdots & \vdots & \vdots \\ \varepsilon_{11}(t_N) & 0 & 0 & 0 & 0 & \varepsilon_{12}(t_N) & \varepsilon_{13}(t_N) & 0 & 0 \\ \varepsilon_{21}(t_N) & 0 & 0 & 0 & 0 & 0 & 0 & \varepsilon_{24}(t_N) & \varepsilon_{25}(t_N) \\ \lambda_{11}(t_N) & \lambda_{12}(t_N) & \lambda_{13}(t_N) & 0 & 0 & 0 & 0 & 0 & 0 \\ \lambda_{21}(t_N) & 0 & 0 & \lambda_{24}(t_N) & \lambda_{25}(t_N) & 0 & 0 & 0 & 0 \\ \rho_{11}(t_N) & \rho_{12}(t_N) & \rho_{13}(t_N) & 0 & 0 & 0 & 0 & 0 & 0 \\ \rho_{21}(t_N) & 0 & 0 & \rho_{24}(t_N) & \rho_{25}(t_N) & 0 & 0 & 0 & 0 \end{bmatrix}$$

Since the identification is in the off-line world, it is sufficiently relevant to have $[q_i(t), \dot{q}_i(t), \ddot{q}_i(t), p_{\pm i}(t), \dot{p}_{\pm i}(t)]$ $(i = 1, 2)$ in every time steps $t = t_1, \cdots, t_N$ by differential approximations. By the projection theorem in Hilbert space, the values a_1 and a_2

$$\hat{a}_1 = \left(X_{1N}^{\mathrm{T}}X_{1N}\right)^{-1}X_{1N}^{\mathrm{T}}Y_{1N}\quad ,\quad \hat{a}_2 = \left(X_{2N}^{\mathrm{T}}X_{2N}\right)^{-1}X_{2N}^{\mathrm{T}}Y_{2N} \qquad (3)$$

are unique [4]. Note that the smaller normal equations consist of the mechanical part and the fluid part and that the bulk modulus b and all of the flow gains $C_\bullet$ are identified explicitly.

The proposed approach is new and applicable to electric robots that stands on the uneven ground with unknown inclination, equivalently, unknown gravity acceleration g.

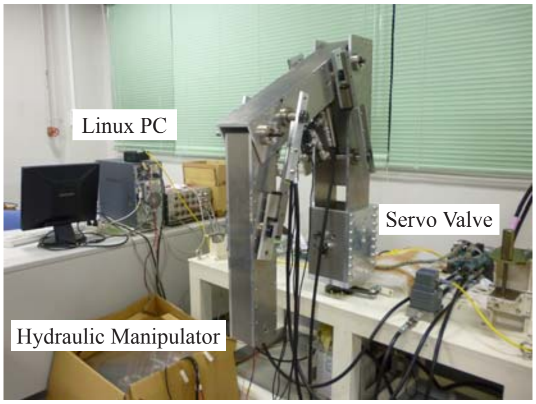

Fig. 4. The experimental setup.

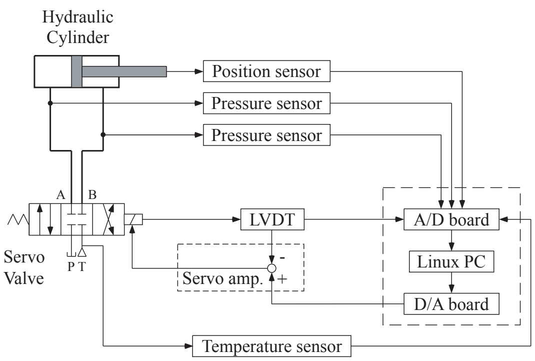

Fig. 5. The system configuration of the hydraulic manipulator.

IV. Identification experiment

A. Method (identification)

Fig.4 shows an appearance of the experimental setup. The experimental setup consists of a vertical and articulated 2-DOF manipulator, a pump (NDR081-071H-30, 11.7 [L/min], $p_s = 7\,[\text{MPa}]$), a tank 7 [L]), four pipes (SWP70-6, 1/4 inch), a valve (KSPS-G02-41-10, direct-type, zero-lap, 40 [L/min], dizzer 300 [Hz]), two cylinders (asymmetric cylinder (KW-1CA30×75, $L = 75\,[\text{mm}]$), a filter (UM-03-20U-1V) and an oil (ISO VG32, $860\,[\text{kg/m}^3]$ $40 \pm 2\,[°C]$). Table II shows the value of the known parameters.

The output signals $p_{\pm i}$ are measured by a pressure sensor (AP-15S), the output s_i is measured by a potentio-meter (LP-100F-C) and the identification input u_{si} are measured by the LVDT (1 [mm]/1.4 [V]). These output and input signals are detected by an AD converter (PCI-3155, 16 bit) and recorded by a control PC (LX7700, Linux, 2.53 [GHz]) by a sampling time 1 [ms]).

In order to identify the parameters, the following control inputs $(v_i = A_i \sin(2\pi f_i t))$are used as the amplitudes $A = 0.5, 1.0\,[\text{V}]$, the frequencies $f = 1.0\,[\text{Hz}]$, the period $t = 6-10\,[\text{s}]$ via DA converter(PCI-3325, 12 bit). Since the parameter identification is in the off-line world, the time derivative of the piston displacement s_i and the pressures $p_{\pm i}$ are sufficiently calculated via the first or second difference approximation and the standard moving average (20-order, cut-off 50 [Hz]). In this paper, all of the identified parameters are from an average of 10 times experiment.

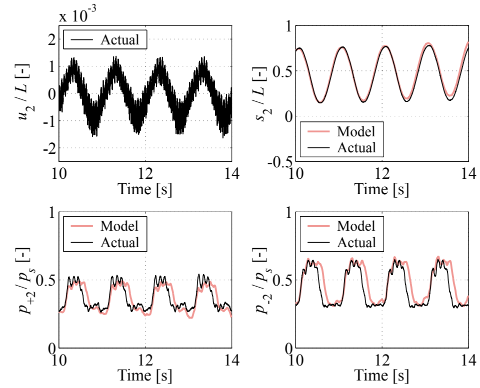

Fig. 6. Model validation (Link 2, Step1, 1.0 Hz).

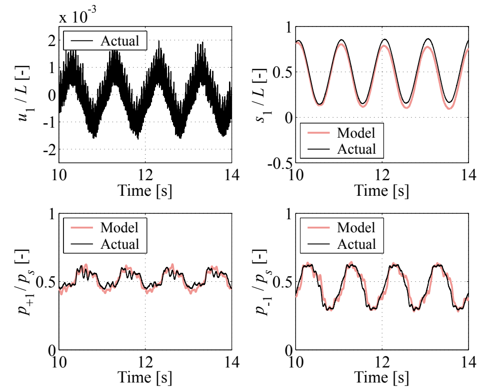

Fig. 7. Model validation (Link 1, Step2, 1.0 Hz).

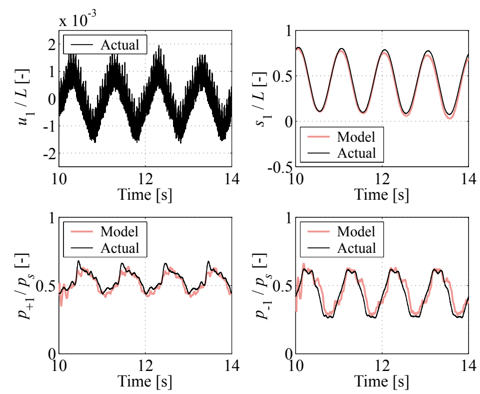

Fig. 8. Model validation (Link 1, Step3, 1.0 Hz).

B. Experimental results (identification)

Table III shows the maximum, the minimum and the average of the identified parameters and their relative standard derivation (RSD [%]). The calculation time to solve the equations (3) are 6.5 [s] on a PC (1.67 [GHz]). The condition number of X_{1N}, X_{2N} are 11, 27 at most and 10, 25 at least, respectively, where the number of row is 12000 and 24000. At first, it is remarkable that the all of 16 dimensional parameters in Table III have positive even though we did not give any constraint on the sign and ranges and any initial estimations to solve the equations (3).

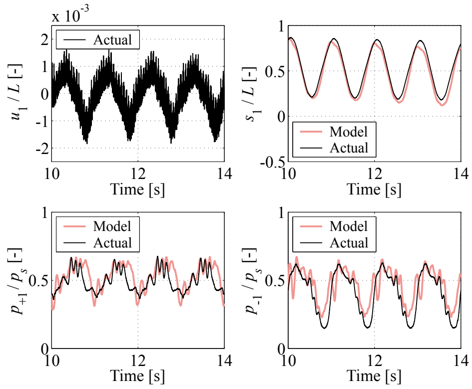

Fig. 9. Model validation of simultaneous motion (Link 1, 1.0 Hz).

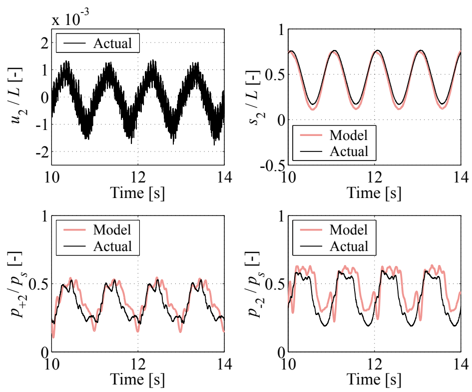

Fig. 10. Model validation of simultaneous motion (Link 2, 1.0 Hz).

To our knowledge, from the viewpoint of robotics, this is the first paper to identify the full parameters without trial and error in case of hydraulic robots. The conventional approaches have identified a part of the parameters by trial and error and are less scientific. The result is directly applicable to impedance controls and the recursive version of the equations (3) will be used adaptive control and so on. From the viewpoint of automation, the result is also important because the spool is the direct type and thus similar to the one of industrial excavators. This paper has opened many doors to model based control of such excavators.

C. Discussion (identification)

Since RSD in Table III are 2.15 [%] at most and 0.14 [%] at least and smaller than 5.00 [%] which is acceptable value in general situation. The condition numbers are less 27 and sufficiently small. Table III also shows the nominal values. In mechanical part, the nominal values are from the mechanical design draft. The friction parameters of the mechanical part and the parameters in fluid part have no good nominal values. However, the bulk modulus value is very close to the result in the paper [8] whose supply pressure p_s is the same as that in this paper. The RSD of the bulk modulus is not small but reliable because the oil temperature is not completely fixed. In these senses, the results are reliable.

V. Model validation

A. Method (model validation)

The equation (1) with the identified parameters is the nonlinear model. This model is quite useful since the model can be used for dynamical simulation with well initial conditions, the optimization design. The model is also useful to estimate the endpoint force because the equation (1) has not endpoint force.

This section discusses the cross validation. That is, the validity of the constructed model is confirmed by the new data which is not used in the identification. This cross validation is fair and also scientific because the conventional approaches use the same data as used in their identification.

First a nonlinear model is constructed in the PC (1.67 [GHz], Simulink) with the average of the result. Second, via Runge − Kutta method (ode45, variable step), the experimental output signals and the model output signals are generated by the same input signals $t = 10 - 14$ [s] and are compared with each other. The initial values of the model is from the experimental states at the start time $t = 10[s]$ except the piston velocity $\dot{s}(0)$ which is replaced by the first-order differentiation. Also, the model validation is repeated by a new input with the frequency $f = 3.0$ [Hz] which is not used in the identification at all.

B. Experimental result (model validation)

Figs.6-8 shows the result in the frequency $f = 1.0$ [Hz]. The result in the frequency $f = 3.0$ [Hz] are omitted here. The black lines denote the experimental inputs and outputs. The red lines denote the model outputs generated by the experimental inputs. In these figures, the inputs and the outputs are normalized by $L(= 75\,[\text{mm}])$ or $p_s(= 7\,[\text{MPa}])$. First, in both frequencies, $f = 1.0 3.0$[Hz], the state equation has the solution successfully. That is, unlike in case of search methods (PSO and GA), the all terms of the state equation are always real number and never the complex number. Second, with respect to the amplitude and the phase, the experimental outputs and the model outputs are very close to each other. Table IV shows the FIT ratio [%]. In general, the FIT ratio can be negative but the results are always positive remarkably.

C. Discussion (model validation)

Figs.6–8 and Table IV imply that the validity of the proposed method is sufficiently acceptable. Especially, a characteristic pressure behavior at every peaks in Fig.6 is seen in both cases. The FIT ratios are quite high and the FIT ratio of the positing velocity are always over 90%.

Even when the endpoint grasps the object with the mass (6.5 [kg]), successfully, only the mechanical parameters R_{12} and W_1,W_2 depending on the endpoint mass has responded. with the condition of the oil temperature (40 ± 2 [°C]) and the frequency $f = 1.0$ [Hz]. Also the identified values are close to the new nominal value of $M_2 = 12.21$ [kgm^2] from the mechanical design draft. On the other hand the fluid parameters are almost same as the case without such load.

TABLE III
IDENTIFIED RESULTS.

Parameter	Symbol	Unit	Proposed Value Min.	Proposed Value Mean	Proposed Value Max.	Proposed RSD [%]	PSO Value	GA Value	Nominal Value
Inertia parameter	M_1	kgm^2	4.43	4.47	4.52	0.52	-	-	5.00
Inertia parameter	M_2	kgm^2	1.25	1.27	1.32	1.71	0.50	3.20	1.00
Inertia parameter	R_{12}	kgm^2	1.33	1.37	1.38	0.94	-	-	1.50
Damping coefficient	F_{v1}	Ns/m	49.79	50.77	51.03	0.74	-	-	-
Damping coefficient	F_{v2}	Ns/m	4.22	4.43	4.51	1.82	1.70	16.36	-
Gravity parameter	W_1	kgm	8.52	8.55	8.60	0.31	-	-	8.60
Gravity parameter	W_2	kgm	3.27	3.30	3.36	0.71	1.33	13.15	3.00
Bulk modulus	$b\,(\times 10^2)$	MPa	2.25	2.33	2.38	2.15	3.17	2.46	$2.00 \sim 17.0$
Flow gain coefficient	$C_{f++1}\,(\times 10^{-7})$	$\mathrm{m}^2/(\mathrm{sV}\sqrt{\mathrm{Pa}})$	6.28	6.31	6.33	0.32	-	-	-
Flow gain coefficient	$C_{f+-1}\,(\times 10^{-7})$	$\mathrm{m}^2/(\mathrm{sV}\sqrt{\mathrm{Pa}})$	6.58	6.60	6.62	0.14	-	-	-
Flow gain coefficient	$C_{f-+1}\,(\times 10^{-7})$	$\mathrm{m}^2/(\mathrm{sV}\sqrt{\mathrm{Pa}})$	5.45	5.50	5.54	0.52	-	-	-
Flow gain coefficient	$C_{f-1}\,(\times 10^{-7})$	$\mathrm{m}^2/(\mathrm{sV}\sqrt{\mathrm{Pa}})$	6.23	6.27	6.32	0.41	-	-	-
Flow gain coefficient	$C_{f++2}\,(\times 10^{-7})$	$\mathrm{m}^2/(\mathrm{sV}\sqrt{\mathrm{Pa}})$	6.26	6.28	6.32	0.34	2.39	6.76	-
Flow gain coefficient	$C_{f+-2}\,(\times 10^{-7})$	$\mathrm{m}^2/(\mathrm{sV}\sqrt{\mathrm{Pa}})$	5.34	5.36	5.39	0.38	2.41	6.17	-
Flow gain coefficient	$C_{f-+2}\,(\times 10^{-7})$	$\mathrm{m}^2/(\mathrm{sV}\sqrt{\mathrm{Pa}})$	5.40	5.44	5.47	0.37	2.38	6.97	-
Flow gain coefficient	$C_{f-2}\,(\times 10^{-7})$	$\mathrm{m}^2/(\mathrm{sV}\sqrt{\mathrm{Pa}})$	6.16	6.19	6.21	0.24	2.43	9.04	-

TABLE IV
FIT RATIO [%].

State	Symbol	Proposed Step 1 1.0 Hz	Proposed Step 1 3.0 Hz	Proposed Step 2 1.0 Hz	Proposed Step 2 3.0 Hz	Proposed Step 3 1.0 Hz	Proposed Step 3 3.0 Hz	PSO Step 1 1.0 Hz	GA Step 1 1.0 Hz
Cylinder displacement	s_1, s_2	91.7	45.8	81.1	45.8	60.9	51.0	-2.4	52.6
Cap pressure	p_{+1}, p_{+2}	33.6	45.5	40.2	67.4	50.7	64.0	5.1	-743.7
Rod pressure	p_{-1}, p_{-2}	35.1	2.8	69.4	47.1	61.3	57.1	-7.2	-1.0×10^4

Figs.9,10 shows the further result where both joint 1 and joint 2 are driven simultaneously with the same frequency $f = 1.0\,[\mathrm{Hz}]$. Unlike electric robots, hydraulic robots have an fluid interaction via energy source (the pump). However, the experimental outputs and the model outputs are close to each other again.

Finally, the proposed approach and the simultaneous approach are compared with the same frequency $f = 1.0\,[\mathrm{Hz}]$. The condition number of the matrix X_{1N}, X_{2N} are 22 and 27 and the value W_1 is larger than the value W_2 which means theoretically impossible. As discussed in above in this paper, the simultaneous identification is restrictive due to the workspace and so on.

In all, the validity of the proposed method is confirmed. The only the proposed method solves the parameter identification without trial and error.

VI. CONCLUSION

This paper is the first report of parameter identificaiton of a hydraulic robot without try and error. Especially the bulk modulus and the all flow gain coefficients are explicitly identified well and the model outputs (the time-response of mechanical displacement and the fluid pressures) and the experimental outputs are very close to each other. All parameters are identified uniquely by projection theorem based on a new discussion of structural properties of hydraulic robots. Every conventional methods need trial and error or looses uniqueness which will cause a kind of trial and error again.

The result is quite important from the viewpoint of both robotics and automation whose valves are normally similar to our direct valves, rather than others (BigDog and so on). This paper opens a new door to model based control, especially impedance control to be implemented in the on-line world. Of course the numerical simulation, design optimization and failure detection are also possible based on this paper.

REFERENCES

[1] Bruno H., G. Barbosa, Luis A. Aguirre, Carlos B. Martinez, and Antonio P. Braga. Black and gray-box identification of a hydraulic pumping system. *IEEE Trans. Control Systems Technology*, 19(2):398–406, 2011.

[2] M. Jelali and A. Kroll. *Hydraulic Servo Systems*. Springer, 2002.

[3] C. Kaddissi, J.-P. Kenne, and M. Saad. Indirect adaptive control of an electrohydraulic servo system based on nonlinear backstepping. *IEEE Transactions on Mechatronics*, 16(6):1171–1177, 2011.

[4] David Luenverger. *Optimization by vector space method*. John Wiley Sons, 1960.

[5] Romain Marion, Riccardo Scorretti, Nicolas Siauve, Marie-Ange Raulet, , and Laurent Krahenbuhl. Identification of jiles atherton model parameters using particle swarm optimization. *IEEE Transactions on Magnetics*, 44(6):894–897, 2008.

[6] H. Mayeda, K. Yoshida, and K. Osuka. Base parameters of manipulator dynamic models. *IEEE Trans. Robotics and Automation*, 6:312–321, 1990.

[7] H. Merrit. *Hydraulic Control Systems*. John Willey & Sons, 1967.

[8] A. Mohanty and Bin Yao. Integrated direct/indirect adaptive robust control of hydraulic manipulators with valve deadband. *IEEE Transactions on Mechatronics*, 16(4):707–715, 2011.

[9] Q. Zhang. *Basics of hydraulic systems*. CRC Press, 2008.

[10] W.H. Zhu and J.C. Piedboeuf. Adaptive output force tracking control of hydraulic cylinders with applications to robot manipulators. *Transactions of the ASME Dynamic systems, Measurement and Control*, 127(1):206–217, 2005.